

LEVEL 12
NOSC

NOSC TR 503

NOSC TR 503

DTIC
ELECTE
JUN 6 1980

Technical Report 503

**ADAPTIVE CANCELLATION OF
MAGNETIC NOISE GENERATED BY
OCEAN SURFACE WAVES**

Dr. G. A. Garcia

15 February 1980

Final Report: July 1979 -- September 1979

Prepared for
Applied Physics Laboratory (APL)
Johns Hopkins Road
Laurel, MD 20810

Approved for public release; distribution unlimited

NAVAL OCEAN SYSTEMS CENTER
SAN DIEGO, CALIFORNIA 92152

80 6 5 0 53

ADA 085127

DDC FILE COPY



NAVAL OCEAN SYSTEMS CENTER, SAN DIEGO, CA 92162

AN ACTIVITY OF THE NAVAL MATERIAL COMMAND

SL GUILLE, CAPT, USN

Commander

HL BLOOD

Technical Director

ADMINISTRATIVE INFORMATION

The work was performed for the Applied Physics Laboratory, Johns Hopkins University, under APL contract 600676 in support of the SSBN Security Technology Program under Navy contract N00024-78-C-5384. This report covers work from 1 July through 30 September 1979.

The author thanks Debra Gookin for her assistance in recording and processing the experimental data.

Released by
I. P. Lemaire, Head
Advanced Systems Division

Under Authority of
H. R. Talkington, Head
Ocean Technology Department

Unclassified

14NOSC/TR-503

SECURITY CLASSIFICATION OF THIS PAGE (When Data Entered)

REPORT DOCUMENTATION PAGE		READ INSTRUCTIONS BEFORE COMPLETING FORM
1. REPORT NUMBER NOSC Technical Report 503 (TR 503)	2. GOVT ACCESSION NO. AD A685 127	3. RECIPIENT'S CATALOG NUMBER 9
4. TITLE (and Subtitle) ADAPTIVE CANCELLATION OF MAGNETIC NOISE GENERATED BY OCEAN SURFACE WAVES		5. REPORT NUMBER AND SERIES Final Report 1 July 39 Sep 79, September 15, 9
6. AUTHOR G. A. Garcia		7. PERFORMING ORG. REPORT NUMBER
8. PERFORMING ORGANIZATION NAME AND ADDRESS Naval Ocean Systems Center San Diego, CA 92152		9. CONTRACT OR GRANT NUMBER(s) APL 600676 in support of Navy contract N00024-78-C-5384.
10. CONTROLLING OFFICE NAME AND ADDRESS Applied Physics Laboratory (APL) Johns Hopkins Road Laurel, MD 20810		11. PROGRAM ELEMENT, PROJECT, TASK AREA & WORK UNIT NUMBERS
12. MONITORING AGENCY NAME & ADDRESS (if different from Controlling Office)		13. REPORT DATE 15 February 1980
		14. NUMBER OF PAGES 1220
		15. SECURITY CLASS. (of this report) Unclassified
		16. DECLASSIFICATION/DOWNGRADING SCHEDULE
17. DISTRIBUTION STATEMENT (of this Report) Approved for public release; distribution unlimited		
18. DISTRIBUTION STATEMENT (of the abstract entered in Block 20, if different from Report) 		
19. SUPPLEMENTARY NOTES 		
20. KEY WORDS (Continue on reverse side if necessary and identify by block number) Ocean Magnetic noise suppression Magnetometers Adaptive noise cancellation Surface wave fields.		
21. ABSTRACT (Continue on reverse side if necessary and identify by block number) A method of suppressing ocean surface wave-generated magnetic noise from near surface-mounted total field magnetometer signals is presented. This technique uses reference data furnished by a measurement of the ocean surface displacement at a single point in the vicinity of the magnetometer to cancel adaptively the magnetic noise generated by the surface wave field. A transfer function is derived which relates the ocean surface displacement measurement to the associated magnetic noise field. Experimental data obtained from a total field magnetometer mounted 7 meters above the ocean surface in approximately 18 meters of water display good correlation with an ocean surface displacement measurement made with a sub-surface-mounted pressure gauge. The transfer function which relates these measurements shows good agreement with the theoretically derived transfer function. When the surface displacement time		

DD FORM 1 JAN 73 1473

EDITION OF 1 NOV 65 IS OBSOLETE
S/N 0102-LF-014-6601

Unclassified

SECURITY CLASSIFICATION OF THIS PAGE (When Data Entered)

393159

[Handwritten signature]

Unclassified

SECURITY CLASSIFICATION OF THIS PAGE (When Data Entered)

series is used as the reference input to an adaptive noise canceller, the surface wave-generated magnetic noise is suppressed by approximately 20 dB at the main swell frequency of 0.08 Hz. Within the frequency band between 0.05 Hz and 0.3 Hz, the degree of cancellation varies between 10 dB and 20 dB.

Accession For	
NTIS	<input checked="checked" type="checkbox"/>
DOC TAB	<input type="checkbox"/>
Unannounced	<input type="checkbox"/>
Justification	<input type="checkbox"/>
By	
Dist	
A	
Dist	A

Unclassified

SECURITY CLASSIFICATION OF THIS PAGE(When Data Entered)

CONTENTS

PROBLEM . . .	2
RESULTS . . .	2
INTRODUCTION . . .	3
THEORY . . .	3
EXPERIMENT . . .	8
Results . . .	9
Conclusion . . .	13
BIBLIOGRAPHY . . .	15

ILLUSTRATIONS

1.	Adaptive noise canceller (ANC) schematic diagram . . .	4
2.	Coordinate system applicable to magnetic field calculation . . .	5
3.	Transfer function computation results . . .	9
4.	Adaptive filter block diagram . . .	11
5.	Plot of rms spectra of magnetometer output . . .	12

TABLE

1.	Notation used in this report . . .	14
----	------------------------------------	----

PROBLEM

Develop a method of suppressing ocean surface wave-generated magnetic noise from near surface-mounted total field magnetometer signals.

RESULTS

Reference data furnished by a measurement of the ocean surface displacement at a single point in the vicinity of the magnetometer were used to cancel adaptively the magnetic noise generated by the surface wave field. A transfer function is derived which relates the ocean surface displacement measurements to the associated magnetic noise field. Environmental data obtained from a total field magnetometer mounted 7 meters above the ocean surface in approximately 18 meters of water displayed good correlation with an ocean surface displacement measurement made with a subsurface-mounted pressure gauge. The transfer function which relates these measurements showed good agreement with the theoretically derived transfer function. When the surface displacement time series was used as the reference input to an adaptive noise canceller, the surface wave-generated noise was suppressed by approximately 20 dB at the main swell frequency of 0.08 Hz. Within the frequency band between 0.05 Hz and 0.3 Hz, the degree of cancellation varied between 10 dB and 20 dB.

INTRODUCTION

One approach to the problem of detection and localization of submerged objects is to take advantage of the magnetic fields generated by iron-bearing material contained within the object of interest. This magnetic signature may be obtained with one of several types of magnetometers whose sensitivities range from about 1 nT* to better than 10^{-4} nT.

To take full advantage of the inherent sensitivity of one of the better instruments, one must be able to cope with a number of noise sources, any one of which may mask the additional capability of a more sophisticated magnetometer.

For a stationary sensor, two noise sources predominate. The first of these components, commonly called 'geomagnetic noise', has its origins in a complicated interaction of the solar plasma with the earth's magnetic field. Charged particles become trapped and circulate in a variety of trajectories, causing rapid variations in the geomagnetic field. Because of its solar origin, this noise component is highly correlated with the 11-year sunspot cycle and is particularly troublesome during peaks in sunspot activity.

In addition to geomagnetic noise, magnetometer measurements made near the ocean surface are subject to the second important noise component, ocean wave noise. The ocean surface is a dynamic interface separating air and electrically conductive seawater. Interaction between the earth's magnetic field and this moving interface induces electric currents in the conductive medium which are responsible for measurable surface-generated magnetic fields. Bergin has computed the magnetic field attributable to surface waves generated by winds of various velocities.¹ According to this calculation, a steady 30-knot wind generates a surface wave field which produces over 1 nT rms of magnetic noise at 100 meters above the surface in a frequency band from dc to 1 Hz. Considerable effort has been directed at characterizing this noise source in an attempt to mitigate its presence and increase the probability of detecting magnetic fields produced by sources below the ocean surface.

This report describes a scheme for eliminating part or all of this surface wave-generated noise component by means of adaptive noise cancellation, with reference data provided by a signal proportional to the ocean surface displacement measured at a single point. An experiment performed at the NOSC Oceanographic Research Tower is reported. Results agree with Weaver's model for ocean surface wave noise generation and demonstrate that significant suppression of this noise is possible.²

THEORY

The adaptive noise canceller (ANC) is diagrammed schematically in figure 1. A signal s combined with uncorrelated noise n_0 forms the input to the primary channel of the ANC. The reference channel receives a second noise component n_1 , which is correlated with n_0 through some linear physical process which may or may not be known. Let this physical process be denoted by the transfer function $T(\omega)$. Optimum cancellation occurs when the

*nT = nanotesla = 10^{-9} weber/m² = 10^{-5} gauss = gamma (γ).

¹Naval Research Laboratory Memorandum Report 2843, Magnetic Variations Caused by Wind Waves, by J. M. Bergin, July 1974.

²Weaver, J. T., Magnetic Variations Associated with Ocean Waves and Swell, Journal of Geophysical Research, v 70, p 1921-1929, 15 April 1965.

adaptive filter takes on the characteristics of a Wiener filter with a transfer function given by

$$W = \frac{S_{xd}}{S_{xx}} \quad (1)$$

where S_{xd} is the cross-power spectrum of the primary and reference inputs and S_{xx} is the power spectrum of the reference. If the reference source contains no signal component and is uncorrupted by noise which is uncorrelated with n_0 , then it can be shown that $W(\omega)$ becomes equal to $T(\omega)$.³ Adjustment of the adaptive filter is effected by a gradient-seeking algorithm which attempts to minimize the total power of the error signal

$$e = s + n_0 - y = s + n_0 - h(t) * n_1(t) \quad (2)$$

where $h(t)$ is the impulse response of the adaptive filter. For our purposes, the primary input consists of a combination of magnetic noise from geomagnetic and wave sources. In a real application, this input may also contain a signal from source of interest under the ocean surface. Into the reference input passes a simultaneous measurement of the ocean surface displacement at a single point in the vicinity of the magnetometer sensor. This information may be obtained from wavestaff or subsurface pressure measurements, optical or radar range measurements, or whatever instrumentation is appropriate to the platform at hand. Notice that magnetic signals arising from sources under the surface pass through the ANC without distortion because they are uncorrelated with the surface displacement reference.

Although the adaptive filter finds the optimum transfer function which minimizes e without regard to the physical relationships leading to $W(\omega)$, it is instructive to derive this expression from basic physical principles. We begin by focussing on a simple, sinusoidal

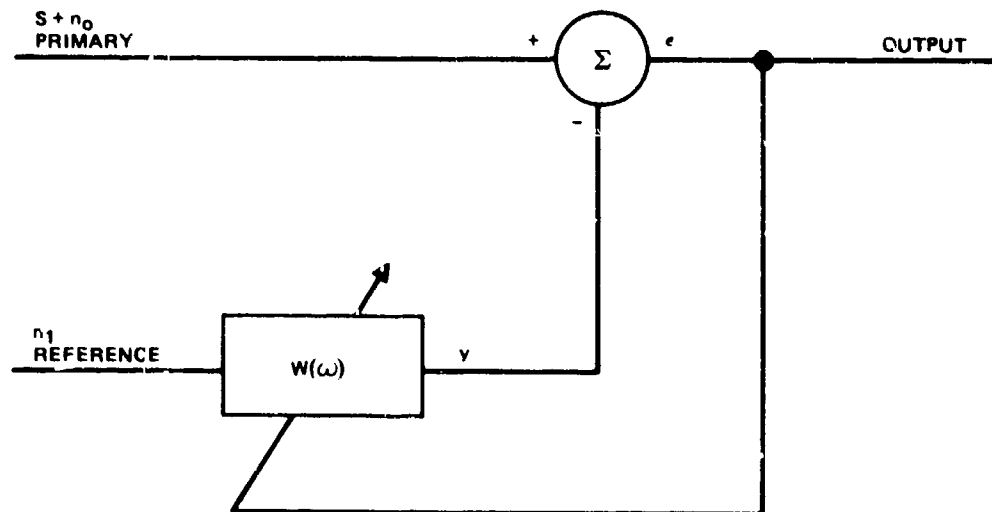


Figure 1. Adaptive noise canceller (ANC) schematic diagram.

³Windrow, B., et al, Adaptive Noise Cancellation: Principles and Applications, Proceedings of the IEEE, v 63, p 1692-1716, December 1975.

ocean surface. Weaver has calculated the magnetic field above and below the surface that is attributable to a monochromatic ocean surface gravity wave in deep water.² A brief condensation of this calculation follows.

Figure 2 shows the coordinate system applicable to this problem and table 1 lists the notation. Initially, let us assume an infinitely deep ocean and therefore ignore bottom effects. The induced electric field in seawater is $\vec{V} \times (\vec{F} + \vec{H})$. The earth's field \vec{F} is enormous compared to the wave-generated field \vec{H} , so that the source term above is just $\vec{V} \times \vec{F}$ to a good approximation. Maxwell's equations for the field vectors may then be written in the form

$$\begin{aligned}\vec{\nabla} \times \vec{E} &= -\partial \vec{H} / \partial t \\ \vec{\nabla} \times \vec{H} &= 4\pi\sigma(\vec{E} + \vec{V} \times \vec{F}).\end{aligned}\quad (3)$$

To solve these equations, the surface velocity field \vec{V} must be specified. Assuming that the ocean medium is incompressible and irrotational, and that the amplitude a of the wave is much smaller than the wavelength, then a monochromatic surface gravity wave moving in a direction θ from the x-axis can be shown to have a velocity given by

$$\vec{V} = -a\omega \left[i(\cos\theta \hat{i} + \sin\theta \hat{j}) + \hat{k} \right] \exp i \left[\omega t - m(x \cos\theta + y \sin\theta) \right] \exp(-mz) \quad (4)$$

where $m = \omega^2/g$. This surface velocity field is inserted in equation 3 and solutions are found which are harmonic in time and displacement for regions above and below the surface. Boundary conditions are then applied to these solutions which require that the normal and tangential magnetic field components be continuous across the air-sea interface. Ultimately, this procedure leads to a harmonically varying magnetic field whose component in the direction of the earth's field (as measured by a total field magnetometer) is given by

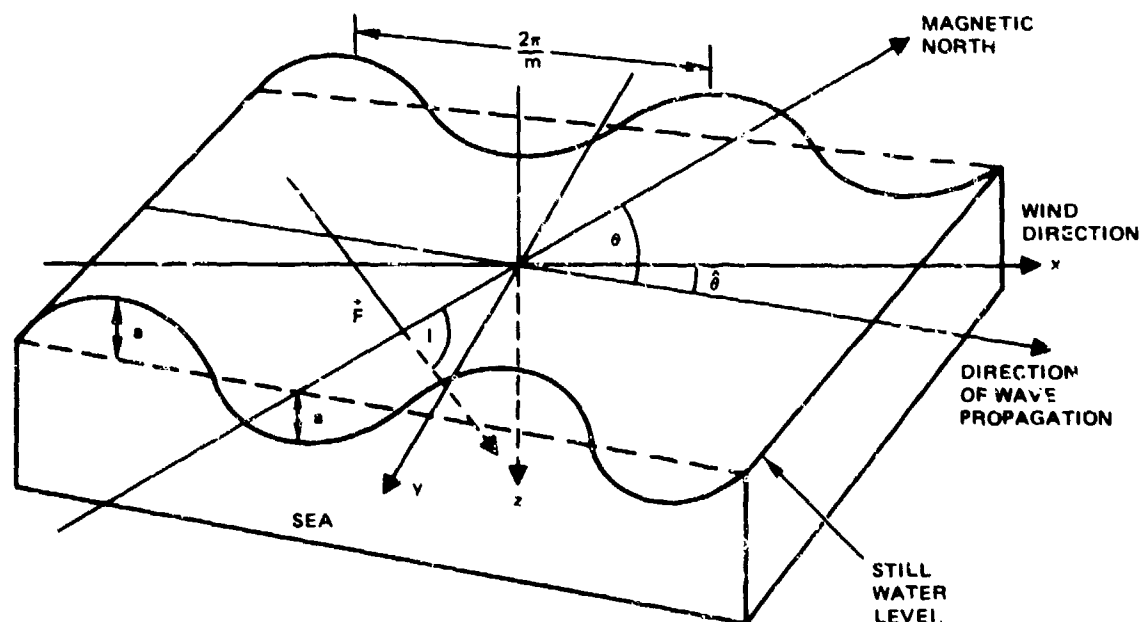


Figure 2. Coordinate system applicable to magnetic field calculation.

$$b_{\parallel} = \frac{-i\pi\sigma g F}{\omega} (S^2 + C^2) e^{-s\omega^2/g} e^{i[\omega t - m(x\cos\hat{\theta} + y\sin\hat{\theta})]} \quad (5)$$

where we have introduced the following notation:

$S = \sin I$: I = dip angle of the earth's field

$C = \cos I \cos \theta$: θ = eastward inclination of wave propagation from the magnetic meridian

s = height of magnetometer above still water level.

b_{\parallel} is Weaver's expression for the magnetic disturbance attributable to a perfectly sinusoidal ocean surface. Of course, the real ocean surface is a complicated superposition of travelling waves of variable frequency, amplitude, phase, and direction of propagation. Equation 5 provides the magnetic disturbance associated with each member of this superposition. By means of a complete specification of the surface directional spectrum, one may proceed to determine the total magnetic field attributable to an arbitrary surface.

Following Pierson's treatment of the ocean surface as a stochastic system, we write the surface displacement in the form

$$p(x,y,t) = \int_{-\infty}^{\infty} \int_{-\pi}^{\pi} \exp i [\omega t - m(x\cos\hat{\theta} + y\sin\hat{\theta}) - \tau(\omega,\hat{\theta})] \cdot \sqrt{[A(\omega,\hat{\theta})]^2} d\hat{\theta} d\omega \quad (6)$$

where $\tau(\omega,\hat{\theta})$ is a phase randomly chosen within the range 0 to 2π and $[A(\omega,\hat{\theta})]^2$ is the directional spectrum of the sea surface.⁴ From equation 5, which gives the magnetic field component parallel to the earth's field attributable to an elemental wave of amplitude a , we can construct a similar elemental field arising from wavelets of the type used to form $p(x,y,t)$:

$$b'_{\parallel} = \frac{-i\pi\sigma g F}{\omega} (S^2 + C^2) e^{-s\omega^2/g} e^{i[\omega t - m(x\cos\hat{\theta} + y\sin\hat{\theta}) - \tau(\omega,\hat{\theta})]} \cdot \sqrt{[A(\omega,\hat{\theta})]^2} d\hat{\theta} d\omega \quad (7)$$

Summing all such contributions, we obtain the total parallel magnetic field component generated by $p(x,y,t)$:

$$B_{\parallel}(x,y,t) = \int_{-\infty}^{\infty} \int_{-\pi}^{\pi} \frac{-i\pi\sigma g F}{\omega} (S^2 + C^2) e^{-s\omega^2/g} e^{i[\omega t - m(x\cos\hat{\theta} + y\sin\hat{\theta}) - \tau(\omega,\hat{\theta})]} \cdot \sqrt{[A(\omega,\hat{\theta})]^2} d\hat{\theta} d\omega \quad (8)$$

As mentioned previously, the reference input to the ANC is proportional to $p(x,y,t)$. The primary input contains the noise component represented by $B_{\parallel}(x,y,t)$ in addition to

⁴Pierson, W. J. Jr., Wind Generated Gravity Waves, Advances in Geophysics, v2, p 93-178, 1955.

other, uncorrelated noise components. Cancellation of $B_f(x, y, t)$ is optimized when the adaptive filter assumes the Wiener transfer function given by equation 1. In this case, the power spectrum of the reference input is just the power spectrum of the surface displacement measurement $p(x, y, t)$, which may be obtained by first forming the autocorrelation function:

$$\langle p(x, y, t) p^*(x, y, t + \lambda) \rangle = \int_{-\infty}^{\infty} \int_{-\pi}^{\pi} [A(\omega, \hat{\theta})]^2 e^{-i\omega \lambda_d} d\omega d\hat{\theta} \quad (9)$$

where we have assumed that $[A(\omega, \hat{\theta})]$ represents a spatially homogeneous and temporally stationary wave field. According to Pierson, et al, $[A(\omega, \hat{\theta})]$ can generally be expressed as a product of a frequency-dependent factor and a direction-dependent factor.⁵

$$[A(\omega, \hat{\theta})]^2 = f(\omega) \cos^2 \hat{\theta} ; \begin{cases} -\infty < \omega < \infty \\ -\pi/2 < \hat{\theta} < \pi/2 \end{cases} \\ 0 ; \text{ otherwise} \quad (10)$$

where the wind direction coincides with $\hat{\theta} = 0$. Integrating the autocorrelation function over $\hat{\theta}$, using the general form for $[A(\omega, \hat{\theta})]$ given in 10, and taking the Fourier transform yields the power spectrum of the reference input:

$$S_{pp} = \pi/2 f^2(\omega) \quad (11)$$

Similarly, the primary and reference cross-power spectrum, S_{pm} , may be calculated from the cross-correlation function of the surface displacement time series, equation 6, and the wave-generated magnetic field time series, equation 8:

$$\langle p(x, y, t) B_f^*(x', y', t' + \lambda) \rangle =$$

$$\int_{-\infty}^{\infty} \int_{-\pi}^{\pi} \frac{i\pi\sigma g F}{\omega} (S^2 + C^2) e^{-s\omega^2/g} e^{-i\vec{k} \cdot \vec{r}} [A(\omega, \hat{\theta})]^2 e^{-i\omega \lambda_d} d\omega d\hat{\theta}$$

$$\text{where } \vec{k} \cdot \vec{r} \equiv \frac{\omega^2}{g} [(x - x') \cos \hat{\theta} + (y - y') \sin \hat{\theta}] \quad (12)$$

The factor $e^{-i\vec{k} \cdot \vec{r}}$ in 12 accounts for the possibility that the displacement measurement may not be taken at the same point in the xy plane as the magnetic measurement. Fourier transformation of the cross-correlation function gives the cross-power spectrum of the reference and primary inputs:

⁵U. S. Navy Hydrographic Office Publication 603, Practical Methods for Observing and Forecasting Ocean Waves by Means of Wave Spectra and Statistics, by W. J. Pierson Jr., G. Neumann, and R. W. Jones, 1955.

$$S_{pm} = \int_{-\pi/2}^{\pi/2} \frac{i\sigma g F}{\omega} (S^2 + C^2) e^{-s\omega^2/g} e^{-i\vec{k} \cdot \vec{r}} \cos^2 \theta f^2(\omega) d\theta \quad (13)$$

where the general form for $[A(\omega, \theta)]^2$ given in 10 has been used. The optimal transfer function is then given by

$$\frac{S_{pm}}{S_{pp}} = \frac{2i\sigma g F}{\omega} e^{-s\omega^2/g} \int_{-\pi/2}^{\pi/2} (S^2 + C^2) e^{-i\vec{k} \cdot \vec{r}} \cos^2 \theta d\theta \quad (14)$$

Any slow variation in the parameters which specify this transfer function will be sensed by the ANC, and the adaptive algorithm will adjust the transfer function of the adaptive filter to accommodate these variations. This feature is particularly important in operational settings where the magnetometer sensor heights may change or the directional characteristics of the wave field may change.

EXPERIMENT

To test the suitability of adaptive noise cancellation techniques to the reduction of wave-generated magnetic noise, an experiment was conducted at the NOSC Oceanographic Research Tower located about 1 mile off the Southern California coast near San Diego. Ordinarily, sensitive magnetic measurements of this type are hampered by stray fields generated by steel in the tower structure. At this facility, however, the magnetometer sensor may be mounted approximately 20 meters from the tower on a non-magnetic boom made of aluminum and glass fiber. This separation provides sufficient magnetic isolation from the tower structure, and tests with sensitive accelerometers have demonstrated that boom motion is negligible in all but the severest sea states.⁶

Two parallel time records were obtained. One time record monitored the total magnetic field as measured by an AN/ASQ-81 optically pumped, metastable, helium magnetometer mounted 7 meters above the surface. This instrument's maximum sensitivity is such that a 0.1-nT full-scale signal produces a 15-volt peak-to-peak output. Under "quiet" geomagnetic conditions, the noise floor of this instrument is less than 0.01 nT. The widest of the selectable passbands was used, giving 3-dB points at 0.04 Hz and 2 Hz. The second time record was a simultaneous measurement of the ocean surface displacement sensed by a pressure transducer located 2 meters below the still water level and 10 meters north of the magnetometer sensor head.

⁶Podney, W., and R. Sager, Measurement of Fluctuating Magnetic Gradients Originating from Oceanic Internal Waves, Science, v 205, p 1331-1382, 28 September 1979.

RESULTS

The Weaver transfer function (equation 14) was derived under the assumption that bottom effects could be ignored. Such conditions hold in the open ocean. However, in a coastal environment, where the experimental data were obtained, the presence of the bottom should be included in any theory which hopes to model the physical process responsible for wave-generated magnetic fields.

Modifications to Weaver's theory which account for finite ocean depths have been made by Woods.⁷ His calculation is a straightforward extension of the theory outlined here and need not be described in detail except to say that an additional interface between the conductive seawater and nonconductive ocean floor must be introduced. This modified transfer function is compared here to the experimental data.

Approximately 1 hour of ocean data was used to obtain the experimental values for the transfer function. The surface displacement record was divided into eight consecutive, nonredundant segments of 400 seconds in length. For each 400-second segment, a windowed Fourier transform was computed. The eight modified periodograms thus obtained were then averaged to give an estimate of the power spectrum of the surface displacement. An estimate of the cross-power spectrum of the surface displacement and the magnetometer measurements was obtained in a similar fashion and the resulting transfer function was computed. The results appear in figure 3, where the solid points represent the experimental

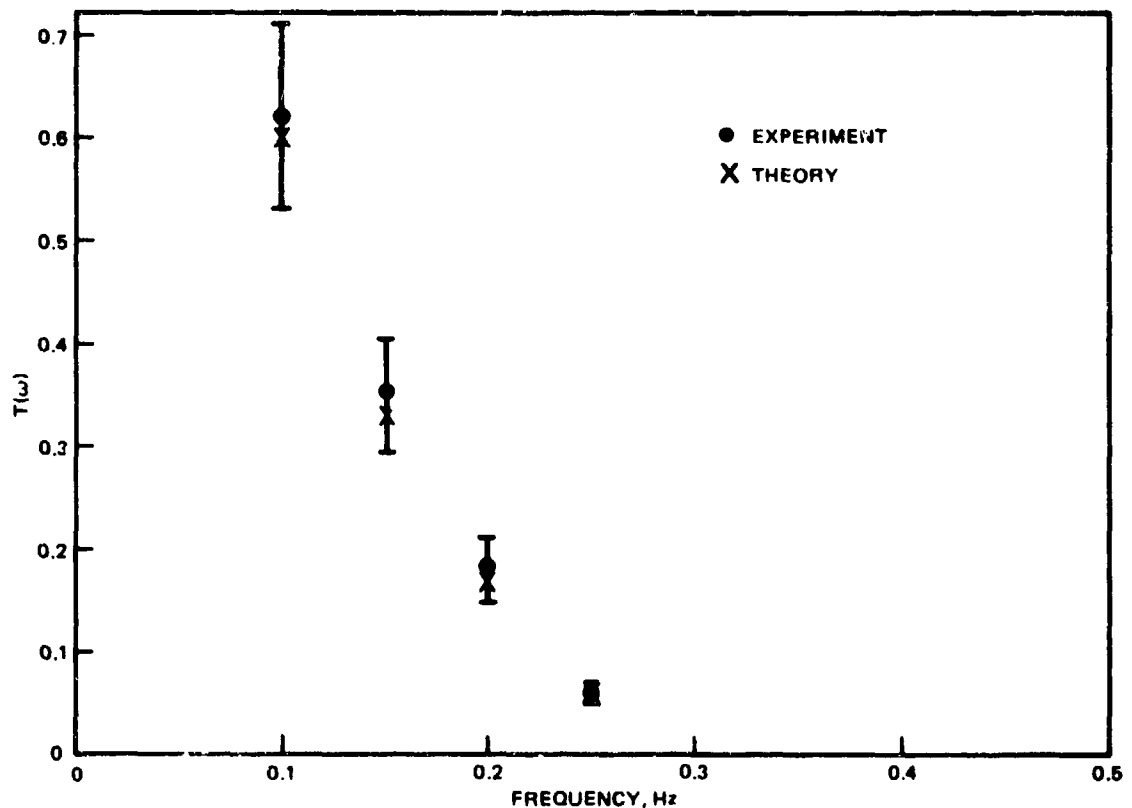


Figure 3. Transfer function computation results.

⁷Defense Research Establishment Pacific, Victoria, B. C. (Canada), PNL Laboratory Note 65-6, Magnetic Variations Associated with Ocean Waves and Swell in a Shallow Sea, by R. S. Woods, July 1965.

transfer function. Each point is an average of the transfer function over a frequency range which spans 0.025 Hz on either side of the point.

Plotted on the same axes is the theoretical transfer function of Weaver modified according to Woods to account for shallow water. For the purposes of this calculation, the following parameters were used:

$$\begin{aligned} l &= 60^\circ \\ \sigma &= 4 \times 10^{-11} \text{ emu} \\ g &= 980 \text{ cm/s}^2 \\ s &= 700 \text{ cm} \\ F &= 50000 \text{ nT} . \end{aligned}$$

In addition, the wave vector of each travelling wave component of the surface displacement was assumed to be refracted normal to the shoreline. Thus, $\theta = 90^\circ$ to a good approximation. The agreement between this theory and the experimental data is well within the error of the measurements.

With the connection between the surface displacement and the associated magnetic field well established, the next step was to determine the extent to which this magnetic noise could be modeled by the adaptive filter from reference data provided by a signal proportional to the surface displacement measured at a single point. The ocean data were processed with a Rockwell Universal Adaptive Filter, which is a digital implementation of the ANC in figure 1. A full description of the LMS adaptive filter, the heart of the ANC, can be found in the extensive literature on this subject (eg, McCool and Widrow).⁸ Very briefly, the adaptive filter consists of a tapped delay line connected to the inputs of an adaptive linear combiner. The adaptive filter is shown in block diagram form in figure 4. The filter output at time j , denoted by y_j , is the discrete convolution of the input vector

$$\tilde{x}_j = (x_j, x_{j-1}, \dots, x_{j-n+1}) \quad (15)$$

where the components of this vector are delayed samples of the input signal x_j , and the weight vector

$$\tilde{w}_{ij} = (w_{1j}, w_{2j}, \dots, w_{nj}) \quad (16)$$

This convolution yields the filter output

$$y_j = \sum_{i=1}^n w_{ij} x_{j-i+1} .$$

Thus the weight vector is a sampled representation of the impulse response of the adaptive filter. The real-time length of the tapped delay line determines the maximum impulse response length of the filter. Within this limit, the filter may assume whatever impulse response minimizes the error e_j . Adaptation of the weight vector is achieved with the LMS

⁸NUC TP 530, Principles and Applications of Adaptive Filters: A Tutorial Review, by J. M. McCool and B. Widrow, March 1977.

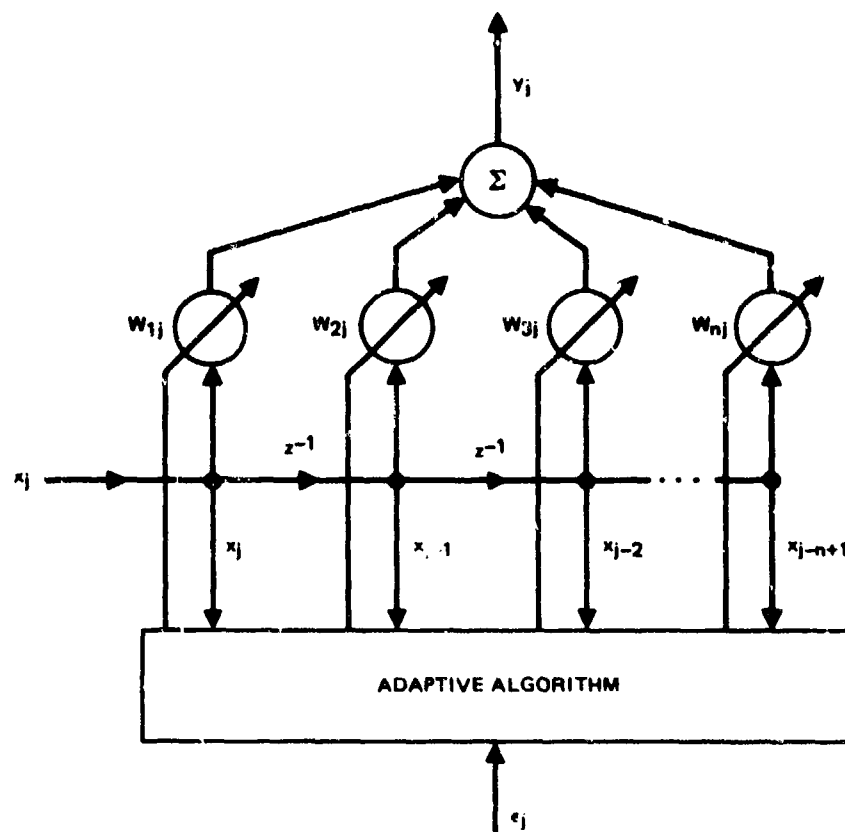


Figure 4. Adaptive filter block diagram.

algorithm which updates the weights according to the prescription given by the following expression:

$$\tilde{W}_{j+1} = \tilde{W}_j + 2\mu e_j \tilde{x}_j. \quad (17)$$

μ , the adaptive feedback constant, influences the rate at which the filter attains the optimal impulse response.

Several filter lengths were used. The filters contained from 64 to 512 taps which represents, at a sample rate of 5.8 Hz, a real-time filter length of 11 to 88 seconds. Within this range, the extent of wave noise cancellation peaked broadly when the filter consisted of about 200 taps, which corresponds to a real-time length of 35 seconds. With the weights initially zeroed, approximately 5 minutes was required for the weight vector to converge to a stationary solution. Figure 5 is a plot of the rms spectra of the magnetometer output before (solid line) and after (dashed line) cancellation. These plots are taken from data processed with a 256-tap filter and $\mu = 2^{-8}$. Throughout the frequency range from 0 to 0.3 Hz, where most of the surface wave spectral power is located, the level of noise suppression averaged about 10 – 15 dB. At the main swell frequency, about 0.08 Hz, the wave-generated noise was suppressed by about 20 dB. Residual noise can be attributed to sources other than surface waves, with the bulk of the unsuppressed noise coming from geomagnetic sources.

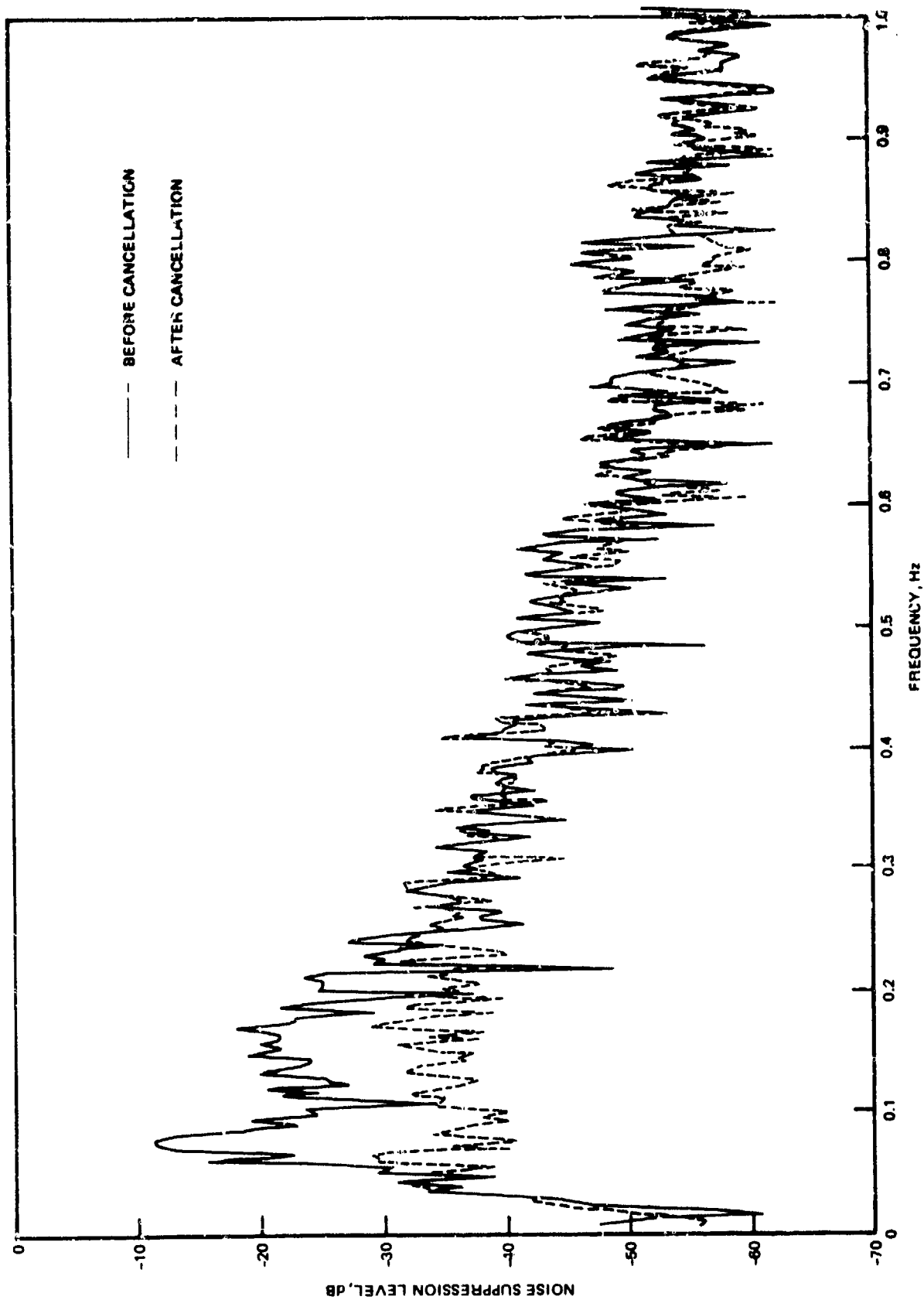


Figure 5. Plot of rms spectra of magnetometer output.

CONCLUSION

The results presented here demonstrate that ocean surface wave-generated magnetic noise may be significantly suppressed by an adaptive noise cancellation scheme which uses reference data furnished by a signal proportional to the surface displacement. Magnetic signals originating from subsurface sources are not expected to be affected by this noise-reduction technique since the reference data are related solely to ocean surface behavior.

Although the surface wave data used in this test were characteristic of coastal waters, it is clear from the Weaver theory that similar measurements made in the open ocean ought to give the same level of noise cancelling performance. In the deep ocean, an area of several thousand square miles may be dominated by the same wind conditions. This property ensures that the adaptive filter transfer function will be time-invariant on a scale which is long compared to the filter adaptation time.

z	Amplitude of ocean wave at the surface
$f^2(\omega)$	Frequency spectrum of the sea surface
$[A(\omega, \theta)]^2$	Directional spectrum of the sea surface
$C = \cos I \cos \theta$	
\vec{F}	Earth's magnetic field
g	Gravitational acceleration
I	Dip angle
$m = \omega^2/g$	
$S = \sin I$	
s	Height of magnetometer sensor above still water level
S_{pr}	Power spectral density of ocean surface displacement measured at one fixed point
S_{pm}	Cross-power spectrum of ocean surface displacement and magnetometer output
θ	Eastward inclination of direction of wave propagation from magnetic meridian
$\hat{\theta}$	Eastward inclination of direction of wave propagation from wind direction
σ	Electrical conductivity
h_s	Magnetic field parallel to the earth's field attributable to a sinusoidal ocean surface
B_f	Magnetic field parallel to the earth's field attributable to an arbitrary surface
p	Surface displacement
$T(\omega)$	Transfer function relating surface displacement to magnetic disturbance

Table 1. Notation used in this report.

BIBLIOGRAPHY

- ¹Naval Research Laboratory Memorandum Report 2843, Magnetic Variations Caused by Wind Waves, by J. M. Bergin, July 1974.
- ²Weaver, J. T., Magnetic Variations Associated with Ocean Waves and Swell, Journal of Geophysical Research, v 70, p 1921-1929, 15 April 1965.
- ³Windrow, B., et al, Adaptive Noise Cancellation: Principles and Applications, Proceedings of the IEEE, v 63, p 1692-1716, December 1975.
- ⁴Pierson, W. J. Jr., Wind Generated Gravity Waves, Advances in Geophysics, v 2, p 93-178, 1955.
- ⁵U. S. Navy Hydrographic Office Publication 603, Practical Methods for Observing and Forecasting Ocean Waves by Means of Wave Spectra and Statistics, by W. J. Pierson Jr., G. Neumann, and R. W. Jones, 1955.
- ⁶Podney, W., and Sager, R., Measurement of Fluctuating Magnetic Gradients Originating from Oceanic Internal Waves, Science, v 205, p 1381-1382, 28 September 1979.
- ⁷Defense Research Establishment Pacific, Victoria, B. C. (Canada), PNL Laboratory Note 65-6, Magnetic Variations Associated with Ocean Waves and Swell in a Shallow Sea, by R. S. Woods, July 1965.
- ⁸NUC TP 530, Principles and Applications of Adaptive Filters: A Tutorial Review, by J. M. McCool and B. Windrow, March 1977.

INITIAL DISTRIBUTION

**THE JOHNS HOPKINS UNIVERSITY
APPLIED PHYSICS LABORATORY
JOHNS HOPKINS ROAD
LAUREL, MD 20810
P. FUECHSEL**

**TRIDENT REFIT FACILITY, BANGOR
CODE 340 (P. MC CARDELL)**

DEFENSE TECHNICAL INFORMATION CENTER (12)